Scattering and energization by large-amplitude whistler-mode waves in the evolution of solar wind electron distributions and Hamiltonian analysis of resonant interactions.

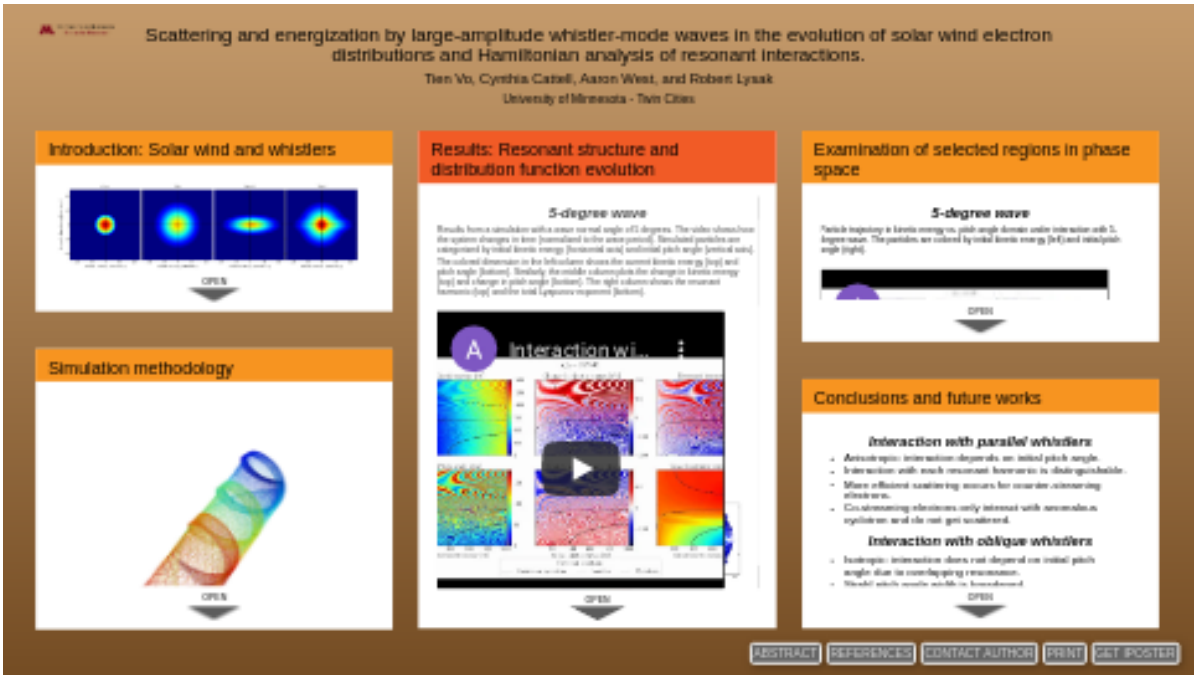

Tien Vo, Cynthia Cattell, Aaron West, and Robert Lysak

University of Minnesota - Twin Cities

PRESENTED AT:

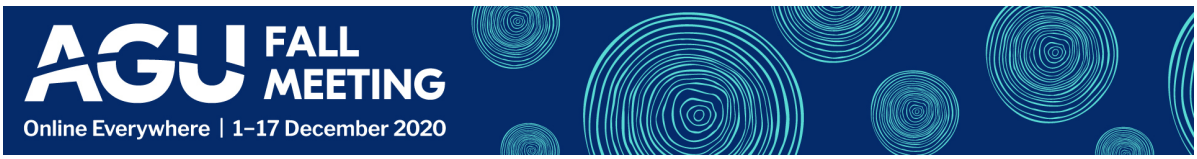

INTRODUCTION: SOLAR WIND AND WHISTLERS

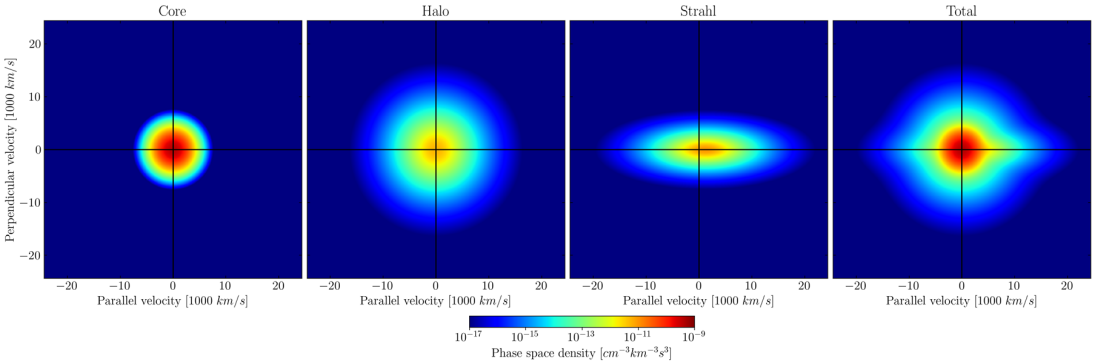

Figure 1. A typical electron distribution seen by the Wind satellite. This is a reconstructed plot using fit parameters from a statistical study by Wilson et. al. (2019).

The solar wind

Solar wind electrons include the **cold core, hot halo, and magnetic field-aligned strahl populations**. Figure 1 shows a model distribution based on Wilson et al. (2019), showing from left to right, the core, halo, strahl and total distributions. **Strahl electrons are expected to remain narrow in pitch angle and field-aligned** as they propagate outward from the Sun due to the conservation of the magnetic moment. **However, in-situ data shows strahl pitch angle widths from 5 to 90 degrees (Anderson et al., 2012)**. The radial evolution of electron distributions has been examined using data from satellites at radial distances from the Sun ranging from Parker Solar Probe (PSP) inside ~ 0.2 AU (Halekas et al., 2020a, 2020b) to Ulysses at ~ 4 AU ((Štverák et al., 2009). These observations are consistent with the existence of significant wave scattering in addition to collisional effects (Maksimovic et al., 2005; Štverák et al., 2009; Wilson III et al., 2000).

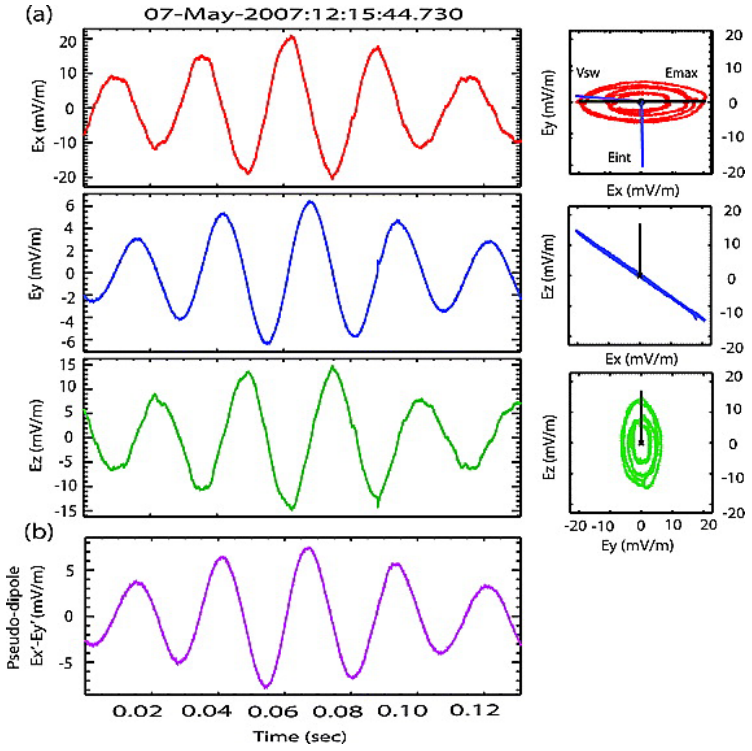

Figure 2. A high amplitude whistler-mode waveform observed on 05/07/2007 by STEREO A (Breneman et. al., 2010).

Whistler-mode waves have long been proposed as a potential mechanism for scattering of solar wind electrons. Theoretical arguments indicated that the waves must propagate sunward to match the resonance condition if the waves propagate parallel to the interplanetary magnetic field. Most theoretical and simulation studies have assumed parallel propagation. Electric field waveform captures from STEREO at 1 AU provided **evidence that large amplitude narrowband whistlers were frequently obliquely propagating, enabling resonant interactions with electrons without the need for sunward propagation** (Breneman et al., 2010; Cattell et al., 2020a). Figure 2 shows one such observational instance of large amplitude whistler (on the order of 10s of mV/m). Similar obliquely propagating whistler-mode waves are observed by PSP inside ~ 0.3 AU (Cattell et al., 2020b; Agapitov et al., 2020).

Our study is designed to assess the role of whistler-mode waves in the scattering and energization of solar wind electrons, using a particle tracing simulation.

Whistler-mode waves

Whistlers are right-hand polarized electromagnetic waves with frequency between the ion and electron cyclotron frequencies. The dispersion relation is given by

$$\frac{c^2k^2}{\omega^2} = 1 - \frac{\omega_{pe}^2/\omega^2}{1-\Omega_c/\omega}$$

Their ability to scatter and energize electrons has been demonstrated by previous simulations using radiation belt magnetic field model (Roth et al, 1999; Hsieh & Omura, 2016, 2017; da Silva et. al., 2018). Breneman et. al., (2010) also observed scattering for electrons in the solar wind magnetic field. The theoretical analysis of the resonant response that leads to these effects using the Hamiltonian formalism is well-established (Albert, 1998, 2000; Tao & Bortnik, 2010; Artemyev et. al., 2018).

$$e^{i\rho\sin\theta} = \sum_{l\in\mathbb{Z}} J_l(\rho)e^{il\theta}$$

Resonant harmonics are orders of the isolated Bessel decomposition term in the Hamiltonian. The resonant condition is

$$l = \frac{\gamma}{\Omega_c}\left(\omega - \frac{k_\parallel p_\parallel}{\gamma m}\right)$$

In our range of interested energy, we observe three harmonics: the cyclotron resonance ($l = 1$), the Landau resonance ($l = 0$), and the anomalous cyclotron resonance ($l = -1$).

We aim to repeat these techniques for simulations of broader spectra of particle distribution and study its evolution in the solar wind conditions.

SIMULATION METHODOLOGY

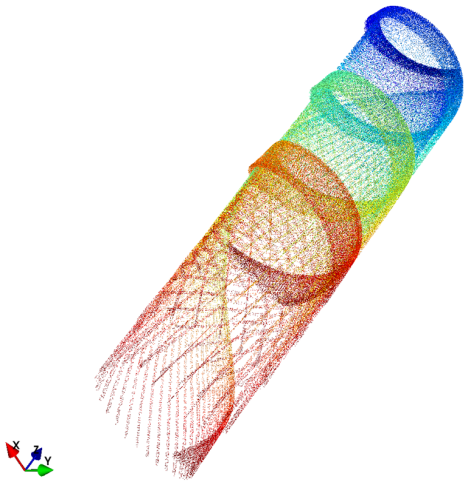

Figure 3. Spatial trajectories of a few hundred particles having initial pitch angle in the range 0-90 degrees in interaction with an anti-parallel whistler wave (the wave propagates towards negative z). The colorscale indicates the flow of time (blue to red).

Simulation parameters based on 1 AU STEREO observations

- Constant background magnetic field.
- Waves propagate in the (xz) plane with various wave normal angles from 5 to 65 degrees. Wave amplitude is large (~10 mV/m) corresponding with $\Delta B/B_0 \sim 0.4 - 0.6$.
- Particles injected at the origin with kinetic energy W_0 and pitch angle α_0.
- Each W_0 and α_0 result is weighted using the distribution shown in Figure 1.

Numerical methods

Equations of motion

We use the **Lorentz force** to derive our equations of motion.

$$\frac{d(\gamma m\vec{v})}{dt} = q(\vec{E} + \vec{v} \times \vec{B})$$

Boris' algorithm, a volume-preserving scheme widely used in Particle-In-Cell simulations, **is used to integrate for the numerical solutions.**

$$\frac{\vec{x}_{n+1} - \vec{x}_n}{\Delta t} = \vec{v}_{n+1}$$

$$\frac{\vec{v}_{n+1} - \vec{v}_n}{\Delta t} = \frac{q}{\gamma m}\left[\vec{E}_n + \frac{(\vec{v}_{n+1} + \vec{v}_n) \times \vec{B}_n}{2\gamma c}\right]$$

Lyapunov exponents

Lyapunov exponents are a measure for "chaos". They determine the extent to which numerical solutions that are originally arbitrarily close diverge from each other. If the Lyapunov exponents are positive, any small perturbation in initial condition results in drastically different solutions, in other words, exponentially increasing distance. Numerical errors are also exponentially increased.

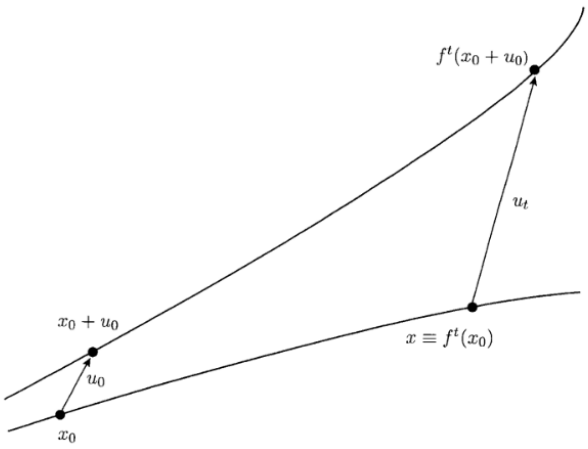

Figure 4. Separation of two phase space trajectories (Sandri, 1996).

We implement a variational approach to estimate the Lyapunov exponents in our dynamical system (Benettin et al., 1980). **A unit volume is attached to the initial position in 6D phase space and its contraction/expansion is calculated from the Jacobian of the Lorentz force**. Figure 4 shows an instance of the expansion in 1 dimension. We use Runge-Kutta of the 4th order to estimate this numerically for local precision. **For each dimension in phase space, the ith Lyapunov exponent is**

$$\lambda_i = \frac{1}{N\Delta t} \sum_{j=1}^{N} \ln ||\overrightarrow{\omega_{j,n}}||$$

where $\overrightarrow{\omega_{j,n}}$ is the principal axis of the parallelpiped in the jth dimension. **Our simulation is then essentially an initial value problem**

$$\frac{d\mathbf{x}}{dt} = \mathbf{F}(\mathbf{x}) \qquad \mathbf{F}(\mathbf{x}_0) = \mathbf{y}_0$$

$$\frac{d\Phi}{dt} = \boldsymbol{\nabla}\mathbf{F} \cdot \Phi \qquad \Phi_0 = \mathbb{1}$$

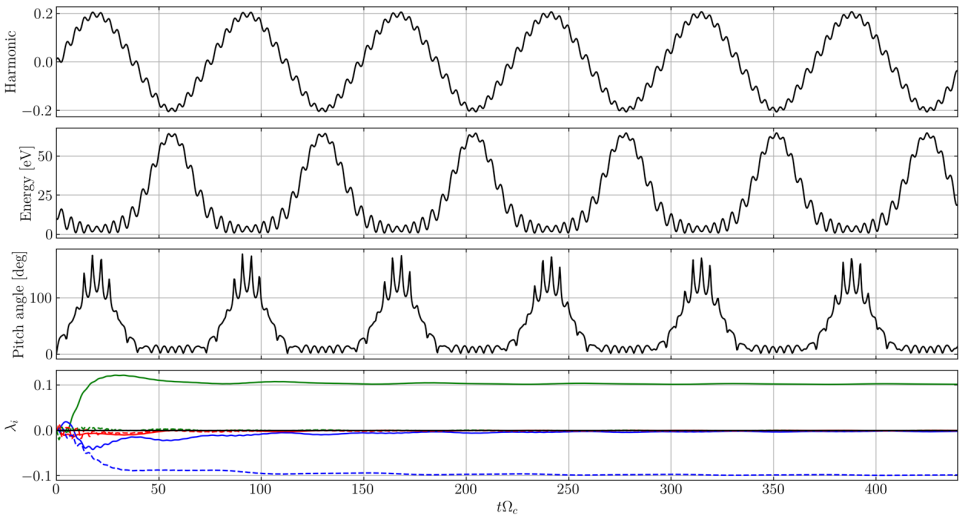

Figure 5. Time series solution for an initially stationary particle at the origin being carried with the inbound whistler (Landau resonance). From top to bottom, the panels show (1) the resonant harmonic, (2) the kinetic energy, (3) the pitch angle, (4) the Lyapunov exponents.

Figure 5 shows a time series of the system's characteristic quantities and the convergence of the Lyapunov exponents in the last panel. **Each of the dimension is unimportant** since the volume is free to rotate in phase space and the algorithm does not take account for that. **However, it is significant whether the total exponent, the extent to which the original unit volume contracts or expands, is reasonably close to zero.** This determines whether our solutions are convergent since Boris' algorithm preserves volume in phase space (Qin et al., 2013). Also, it is interesting to note that **there is at least one chaotic dimension**. **This reflects the resonant interactions when the particle is in the vicinity of a resonant harmonic, where the adiabatic invariant is violated and the system goes through irreversible change.**

RESULTS: RESONANT STRUCTURE AND DISTRIBUTION FUNCTION EVOLUTION

5-degree wave

Results from a simulation with a wave normal angle of 5 degrees. The video shows how the system changes in time (normalized to the wave period). Simulated particles are categorized by initial kinetic energy (horizontal axis) and initial pitch angle (vertical axis). The colored dimension in the left column shows the current kinetic energy (top) and pitch angle (bottom). Similarly, the middle column plots the change in kinetic energy (top) and change in pitch angle (bottom). The right column shows the resonant harmonic (top) and the total Lyapunov exponent (bottom).

[VIDEO] https://www.youtube.com/embed/cU6RfwoiqJQ?rel=0&fs=1&modestbranding=1&rel=0&showinfo=0

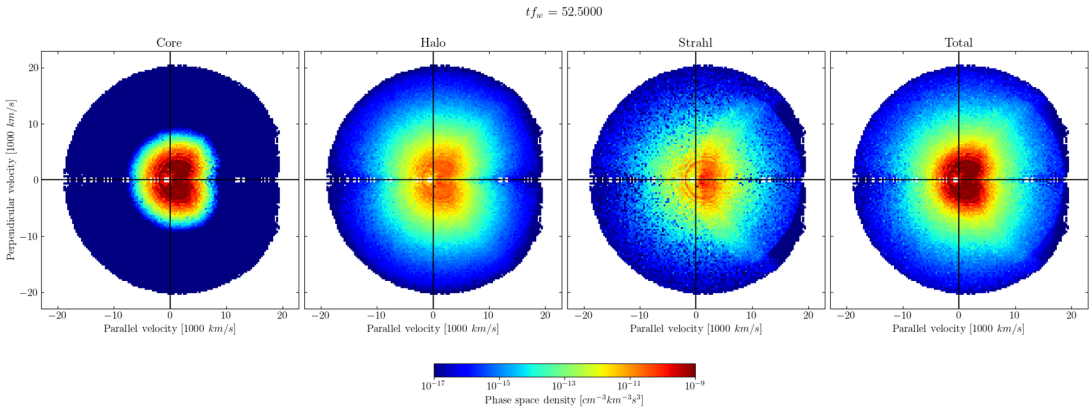

Figure 6. Distribution function after 52 periods of interaction with 5-degree wave.

- Interactions with Landau, cyclotron and anomalous cyclotron resonances cause dramatic changes in both pitch angle and energy.
- For nearly parallel propagating waves, counter-streaming particles (90-180 degrees in pitch angle) are more efficiently scattered. The region of co-streaming electrons (0-90 degrees pitch angle) experiences attracting behavior (negative Lyapunov exponent).
- Strahl angle width is broadened after 52 wave periods.

- Counter-streaming particles are deflected and energized across the co-streaming region, then get scattered back and de-energized by the hard boundary defined by the anomalous cyclotron resonance.

30-degree wave

[VIDEO] https://www.youtube.com/embed/ZLoD7SR5adE?rel=0&fs=1&modestbranding=1&rel=0&showinfo=0

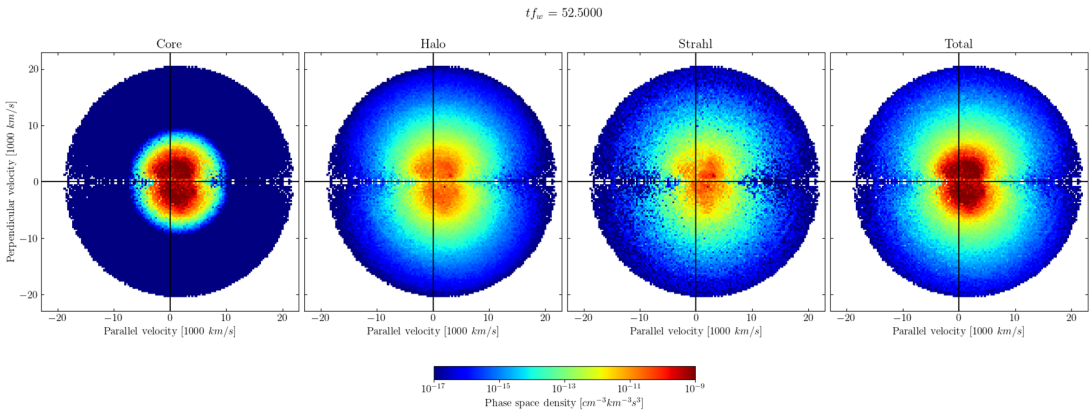

Figure 7. Distribution function after 52 periods of interaction with 30-degree wave.

- Overall less negative Lyapunov exponents. There is no hard scattering boundary.
- Instead of only sunward particles, all particles in the initial distribution interact with all three harmonics. The interaction is isotropic.
- The upper bound in the Lyapunov exponents ensures that this statistical structure is numerically valid (except for the counter-streaming region around 600 eV).
- For obliquely propgating waves (as are seen at 1 AU by STEREO), pitch angle scattering is more efficient.

65-degree wave

[VIDEO] https://www.youtube.com/embed/Sn6lDcw1a5s?rel=0&fs=1&modestbranding=1&rel=0&showinfo=0

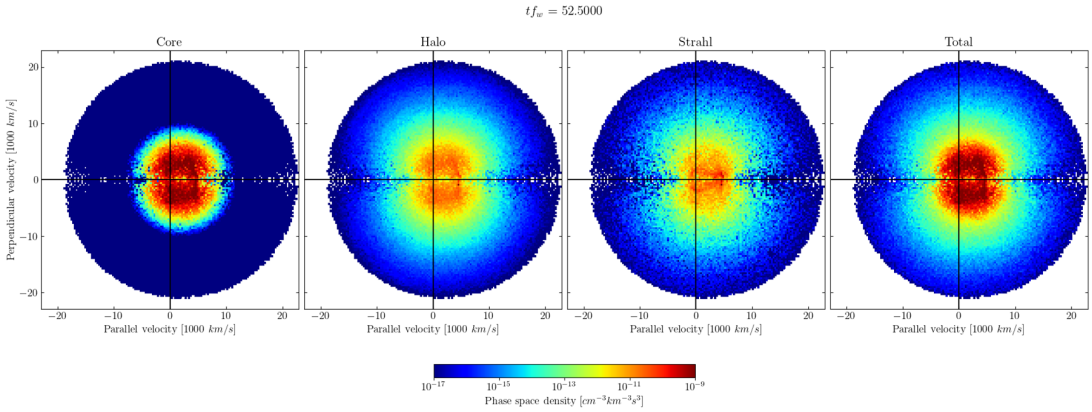

Figure 8. Distribution function after 52 periods of interaction with 65-degree wave.

- Lyapunov exponents are close to zero and there are more chaotic solutions (positive LE).
- Overall, the structure is similar to the 30-degree wave interaction. However, the energization/de-energization is slightly larger.
- Strahl population becomes isotropic. The total population gains a larger drift in the parallel direction.

EXAMINATION OF SELECTED REGIONS IN PHASE SPACE

5-degree wave

Particle trajectory in kinetic energy vs. pitch angle domain under interaction with 5-degree wave. The particles are colored by initial kinetic energy (left) and initial pitch angle (right).

[VIDEO] https://www.youtube.com/embed/Y1JoJi8kb5Q?rel=0&fs=1&modestbranding=1&rel=0&showinfo=0

- Clearly isolated interaction with each harmonic.
- Anomalous cyclotron resonance deflects and scatters particle but does not energize.
- Landau resonance scatters and energizes particles.
- Counter-streaming particles reach steady state slower than particles already in Landau resonance.

30-degree wave

Particle trajectory in kinetic energy vs. pitch angle domain under interaction with 30-degree wave. The particles are colored by initial kinetic energy (left) and initial pitch angle (right).

[VIDEO] https://www.youtube.com/embed/vPdqgFhKzl8?rel=0&fs=1&modestbranding=1&rel=0&showinfo=0

- No distinguishable difference for interaction with each resonance (possibly because of overlapping).
- Interaction does not have a preference in pitch angle. Particles in all ranges of initial energies and pitch angles reach steady state simultaneously and in less than 1 wave period.

65-degree wave

[VIDEO] https://www.youtube.com/embed/R4HowxeITP0?rel=0&fs=1&modestbranding=1&rel=0&showinfo=0

- Similar to 30-degree wave interaction, the response does not have a preference over the range of pitch angles.
- Energization is more significant for more oblique waves.

CONCLUSIONS AND FUTURE WORKS

Interaction with parallel whistlers

- Anisotropic: interaction depends on initial pitch angle.
- Interaction with each resonant harmonic is distinguishable.
- More efficient scattering occurs for counter-streaming electrons.
- Co-streaming electrons only interact with anomalous cyclotron and do not get scattered.

Interaction with oblique whistlers

- Isotropic: interaction does not depend on initial pitch angle due to overlapping resonance.
- Strahl pitch angle width is broadened.
- More efficient energization.

Remaining questions and future works

- Study attractors in the co-streaming region. Why do they disappear (or diminish) for oblique waves?
- Study the bifurcation of steady state over the range of wave normal angles and identify regions of resonance overlap.
- The Hamiltonian analysis for scattering and energization mechanism in the radiation belt assumes isolated harmonics. However, most particles in our distribution interact with either 2 or 3 more harmonic in a short period. A similar analysis needs to be altered without that assumption for a more accurate model of resonant response.
- Modification of the simulation for a wave packet.

ABSTRACT

Whistler-mode waves have often been proposed as a plausible mechanism for pitch angle scattering and energization of electron populations in the solar wind. Theoretical work suggested that whistler waves with wave vectors parallel to the interplanetary magnetic field must counter-propagate (sunward) to the electrons for resonant interactions to occur. However, recent studies reveal the existence of obliquely propagating, high amplitude, and coherent waves consistent with the whistler-mode. Initial results from a particle tracing simulation demonstrated that these waves were able to scatter and energize electrons. That simulation was limited and did not examine a broad range of electron distributions. We have adapted the original particle tracing code for the solar wind with wave parameters observed by the STEREO satellites and to model core, halo and strahl electrons. Simulations are run to record the response of a wide initial phase space volume with uniform waves and wave packets. Using a Hamiltonian analysis, resonant responses at different harmonics of the cyclotron frequency are included in the simulation. A numerical integration scheme that combines the Hamiltonian analysis and the relativistic 3d particle tracing deployed on a high performance cluster enables accurate mapping and large-scale statistical studies of phase space responses. Observations of electron distributions from WIND at 1 AU are used for normalization. This enables extrapolations for core, halo, and strahl electrons evolution with the numerical Green’s function method. Results provide evidence for pitch angle broadening of the strahl and energization of core and halo electrons. This model can also provide results that are applicable to a number of different wave-particle interactions in the heliosphere for comparison to in-situ measurements.

REFERENCES

1. Wilson III L. B. et al., 2019, *ApJS*, 243, 1.
2. Anderson B. R. et al., 2012, *JGR*, 17, A4.
3. Agapitov, O. V., Wit, T. Dudok de, Mozer, F. S. et al., 2020, *ApJ*, 89, L20.
4. Breneman A., Cattell C., Schreiner S. et al., 2010, *JGRA*, 115, A08104.
5. Cattell C., Short, B., Breneman A.W. & Grul P., 2020a, *ApJ*, 897, 126.
6. Cattell C. et al., 2020b, Narrowband oblique whistler-mode waves: Comparing properties observed by Parker Solar Probe at < 0.2 AU and STEREO at 1 AU, submitted to A&A, arXiv:2009.05629v2 [physics.space-ph].
7. Halekas J. S., Whittlesey P., Larson D. E., McGinnis D., Maksimovic M., et al., 2020a, ApJ, 246, 22.
8. Halekas J. S., Whittlesey P., Larson D. E., McGinnis D., Bale S. D. et al., A&A, in press, 2020b.
9. Maksimovic M. et al., 2005, *JGR*, 110, A09104.
10. Štverák, Š., Maksimovic, M., Trávníček, P. M., Marsch, E., Fazakerley, A. N., and Scime, E.E., 2009, JGR 114, A05104.
11. Sandri M., 1996, *The Mathematica Journal*.
12. Benettin G. et al., 1980, *Meccanica*.
13. Qin H. et al., 2013, *Phys. Plasmas*, 20, 084503.